

ANALYTICAL MODELING OF THERMAL RESISTANCE IN BOLTED JOINTS

S. Lee

Aavid Engineering, Inc., Laconia, NH

S. Song, K.P. Moran

Enterprise Systems, IBM Corporation, Poughkeepsie, NY

and M.M. Yovanovich

Department of Mechanical Engineering,
University of Waterloo, Waterloo, Ontario

ABSTRACT

An analytical approximate solution is developed for predicting the thermal resistance of bolted joints between two square plates of the same material but different thicknesses. The plates are assumed to have perfectly flat and smooth surfaces, and they are joined by a bolted connection at the center of the square, forming a concentric annular contact region at the interface. The entire surface area of the plates are insulated, except for the surfaces where the heat source/sink is applied and where the interfacial contact is formed. The heat flows from one edge of a plate to the opposite edge of the other plate through the contact area. The results are presented over a wide range of variables commonly found in most electronic packaging applications. Comparisons with published numerical results show excellent agreement, and satisfactory to good agreement is obtained between the analytical predictions and experimental data.

NOMENCLATURE

a	bolt-hole radius, m
b	plate radius, m
c	contact radius, m
d	washer or pressure radius, m
f_c	factor given by Eq. (7)
J_i, Y_i	Bessel functions of the first and second kinds of order i
k	thermal conductivity, W/mK
L	plate dimension, m
q_0, q_2	heat-flux specified surfaces
R	thermal resistance, $^{\circ}C/W$
r	radial coordinate, m

T_0, T_1, T_2 temperature specified surfaces
 t plate thickness, m

Greek Symbols

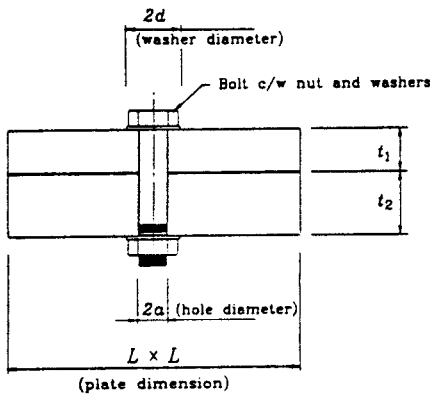
α angle shown in Fig. 2, $\pi/4$
 δ thickness of inner-ring plate, see Eq. (6), m
 λ_n eigen value, m^{-1}
 ϕ_i function defined by Eq. (4)

Subscripts

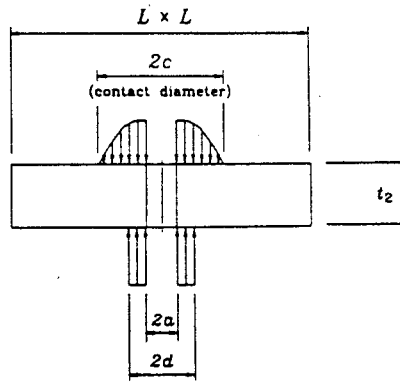
h harmonic mean
 i inner-ring plate
 J joint
 j 1 or 2
 m material
 o outer-ring plate
 t total
1 upper plate
2 lower plate

INTRODUCTION

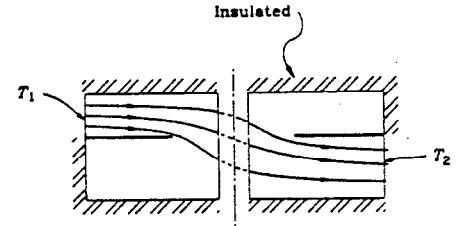
Bolted joint is a simple mechanism commonly found in many parts of electronic equipment. Heat sinks such as liquid cooled cold plates and fins of various shapes and types are often fastened to heat generating electronic components by means of bolted joints. In such assemblies heat is dissipated into a heat sink through a conduction path formed at the interface of the joint, and the performance of a heat sink is directly affected by the geometry and arrangement of bolted joints. As a result, determination of the



a) Schematic



b) Pressure Distribution (Lower Plate)



c) Thermal Problem

Figure 1: Bolted Joint

thermal constriction resistance incurred by having bolted joints becomes an important integral part of the overall design of heat sinks and their attachment.

The analysis of thermal phenomena occurring in a bolted joint is complex as heat flow depends on many independent parameters such as surface roughness, surface waviness, thermal conductivity, Poisson's ratio, yield stress, hardness, applied load, and geometry of the system. In analyzing heat transfer in bolted joints the task can be divided primarily into two components; *i*) mechanical component for determining interfacial pressure distribution and contact size and *ii*) thermal component for determining thermal constriction resistance for given thermal boundary conditions and a contact size.

In earlier studies, conducted by the current authors on thermal contact resistance (Song et al., 1992 and Lee et al., 1993), a bolted joint between two plates of the same material and the same thickness has been investigated. Analytical models have been developed for both mechanical and thermal problems, and simple correlations were developed for accurate estimation of the contact radius and the thermal constriction resistance. In those studies, the thermal problem was composed of two concentric plates fastened by a single bolted joint in the center, and a heat source was assumed to be located on the top plate whereas a heat sink is placed on the bottom plate in such a way that heat flows axisymmetrically down and across the bolted joint. During the past few decades, many other experimental, numerical and analytical investigations have been carried out, as referred to in the aforementioned papers, examining macro as well as micro contact resistances of bolted joints for different geometries and thermal conditions.

In this work, additional model is developed for predicting the total thermal resistance of a bolted joint with a geometry and thermal boundary conditions that have not been previously examined. A schematic of the proposed problem is shown in Fig. 1a. Two

square plates of the same size but different thicknesses, denoted as t_1 and t_2 , are placed in such a way that they overlap each other over the entire square region. The plates are fastened by a bolted connection at the center. The dimensions a and L are the bolt-hole radius and the plate dimension, respectively. Figure 1b shows the lower plate with a schematic representation of the normal pressure distributions at the interface and the bottom surface. The center region of the interface which experiences the compressive pressure represents the contact zone as indicated by the contact radius c in the figure. The pressure distributions for the upper plate are, of course, symmetrical about the interface.

If the two plates are made of the same thickness and the same material then the interfacial contact zone can be predicted closely using the simple correlation equation proposed by Song et al. (1992) and it becomes possible to determine the thermal constriction resistance. On the other hand, if two plates are made of different thicknesses, the interfacial contact area can be estimated from the correlation equation (Song et al., 1993b) which uses the harmonic mean thickness of the two plates.

Figure 1c shows the thermal boundary conditions imposed on the present problem with a schematic representation of the heat flow lines. Heat flows from one end of the assembly to the other end, and both source and sink surfaces are assumed to be maintained isothermal. It is further assumed that the heat loss through all the other exposed surfaces is negligible. The thermal path in the present geometry is not axisymmetrical nor does it conform to any known orthogonal curvilinear coordinate systems. For this reason, exact analytical solution does not exist and an approximate analytical approach is employed to develop a model for predicting the thermal joint resistance. In the following sections, the development of the analytical model is described in detail and comparisons of the predictions with existing finite element numerical data and experimental results are provided.

THERMAL MODELING

Due to the lack of an appropriate orthogonal coordinate system that conforms to the heat flows in the present problem, an approximate analysis will be carried out by modifying the geometry and simplifying the thermal boundary conditions. These approximations would allow us to develop an analytical model and still retain all the essential and fundamental parametric behavior of the problem in the predictions.

The analysis will proceed in two stages. Firstly, the material or bulk resistance of the plates without the constriction effects of the bolted joint will be determined. This resistance is an inherent part of the total joint resistance of a given bolted joint assembly and would become identical to the resistance of the assembly when perfect contact is achieved over the entire square interface. For closed-form analyses, the effects of the bolt hole is ignored in determining the material resistance. Clearly, the material resistance represents the minimum asymptote to which the total joint resistance should approach as the contact area increases for the given system.

The second part of the present investigation deals with the total as well as the constriction resistances due to the annular contact region at the interface. Although the precise thermal condition over the contact zone is not known, the contact surface may be assumed iso-flux as an approximation. This thermal condition closely approximates the limiting condition at the interface as the contact area becomes small. It also allows us to separate the plates and use the same thermal analysis, developed for one plate, for both the upper and lower plates. Furthermore, in order to render the problem to be compatible with known analytical solution techniques, the square plate is modeled approximately as a circular disk with the same thickness and the same surface area as the original plate. This exercise of modifying the problem geometry for the benefit of solution techniques has been often used in the study of contact and constriction resistances (Yovanovich, 1992) and recently employed again with a great success in developing a conduction model for predicting the thermal performance of vias network in a high density interconnect assembly (Lee et al., 1992). The distances from the contacting area to the outer edges of the original square structure are usually large as compared to the contact size, and the resulting thermal resistance of the problem would be insensitive to the actual shape of the outer edges. The outer radius of the disk is determined as such the disk area is maintained identical to the original square area, and the heat source/sink is located over one quadrant of the outer-edge surface of the disk, as depicted in Fig. 2b with $\alpha = \pi/4$.

In addition to the geometric modifications, the isothermal boundary condition prescribed at the edge surface is also replaced by an iso-flux condition. It is well known that, as compared to isothermal conditions, iso-flux conditions will result in higher constriction

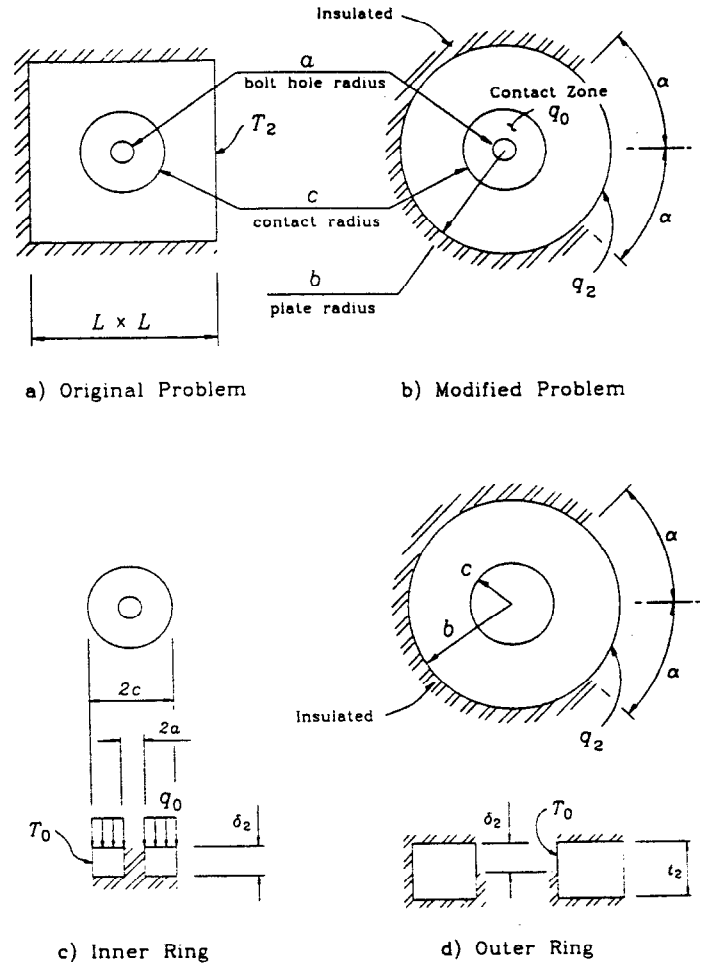


Figure 2: Modeling of Bolted Joint (Lower Plate Shown)

resistances by a nominal factor of 8% (Yovanovich, 1992). For the present problem, this difference of 8% in the constriction resistance becomes no more than 1-3% of the total joint resistance throughout the range of the cases examined herein.

In view of obtaining simple solutions, the thermal problem is further approximated by separating the circular plate into two rings; the inner ring with the inner and outer radii of a and c , and the outer ring with the inner and outer radii of c and b , as illustrated in Figs. 2c and 2d. With an assumed isothermal boundary condition at c , each of these two ring-regions can be solved now by means of the method of separation of variables in two-dimensional, cylindrical coordinates. It is to be noted that the ongoing approximations become closer to the actual conditions if both the interfacial contact area and the plate thickness are small. To account for the effect of thick plates, an adjustment is made in the analysis such that, if the thickness is greater than the contact-ring width ($c - a$), the thickness of the inner-ring plate is made equal to the ring width, and the isothermal boundary condition prescribed at $r = c$ is imposed only over a restricted partial surface area as indi-

cated by δ in Figs. 2c and 2d. Therefore, δ assumes the dimension of the plate thickness or that of the ring width, whichever is less. This is to better account for the actual heat flow path expected in the vicinity of the contact region when the plate thickness is large as compared to the contact-ring width.

In summary, the material resistance obtained in the first stage of the analysis represents an asymptote of the total joint resistance when the contact area is large, and the total resistance determined in the second stage of the analysis represents an asymptote of the actual joint resistance when the contact area is small. These two limiting solutions can be *blended* to yield a comprehensive solution which is valid over the full range of contact radius with correct behaviors at the both limiting conditions.

RESULTS AND DISCUSSIONS

In this section the analytical solutions are presented and the predictions are compared with existing numerical and experimental data. The material resistance of the square plate assembly, schematically shown in Fig. 1a, with a perfect contact over the entire square interface can be accurately predicted from (Yovanovich, 1992)

$$R_m = \frac{1}{k(t_1 + t_2)} - \frac{2}{\pi k L} \left[\ln \left(\sin \left(\frac{\pi}{2} \frac{t_1}{t_1 + t_2} \right) \right) + \ln \left(\sin \left(\frac{\pi}{2} \frac{t_2}{t_1 + t_2} \right) \right) \right] \quad (1)$$

for $L > (t_1 + t_2)$.

Also, as previously described, the method of separation of variables was used in solving the present conduction problems and the following expressions are obtained for the resistances of the inner and outer rings depicted in Figs. 2c and 2d:

$$R_i = \frac{4}{\pi k (c^2 - a^2)^2} \times \sum_{n=1}^{\infty} \frac{1}{\lambda_n^3 \tanh(\lambda_n \delta_j)} \frac{[c\phi_1(\lambda_n c) - a\phi_1(\lambda_n a)]^2}{c^2 \phi_1^2(\lambda_n c) - a^2 [\phi_0^2(\lambda_n a) + \phi_1^2(\lambda_n a)]} \quad (2)$$

$$R_o = \frac{f_c}{2\pi k t_j} \left[\ln(b/c) + \frac{2}{\alpha^2} \sum_{n=1}^{\infty} \frac{\sin^2(n\alpha)}{n^3} \tanh(n \ln(b/c)) \right] \quad (3)$$

where the functions $\phi_0(\cdot)$ and $\phi_1(\cdot)$ are defined by

$$\phi_i(\cdot) = J_i(\cdot)Y_1(\lambda_n a) - J_1(\lambda_n a)Y_i(\cdot) \quad \text{for } i = 1, 2 \quad (4)$$

Here, $J_i(\cdot)$ and $Y_i(\cdot)$ are the Bessel functions of the first and second kinds of order i , respectively, and λ_n is the n -th root of the transcendental equation which satisfies the adiabatic boundary condition at $r = a$ and the isothermal boundary condition at $r = c$:

$$\phi_0(\lambda_n c) = 0 \quad (5)$$

As previously discussed, δ_j , which appears in the above equation for R_i and in the factor f_c expressed below, is the thickness of the inner-ring plate, given as

$$\delta_j = \begin{cases} t_j & \text{if } t_j \leq (c - a) \\ c - a & \text{if } t_j > (c - a) \end{cases} \quad \text{for } j = 1, 2 \quad (6)$$

The factor f_c has been introduced in Eq. (3) to account for the axial-constriction effect which occurs in the outer-ring problem due to the partially imposed isothermal condition at $r = c$ when $t_j > (c - a)$. It is given as

$$f_c = 1 - \frac{2t_j}{\pi(b-c)} \ln \left(\sin \left(\frac{\pi}{2} \frac{\delta_j}{t_j} \right) \right) \quad \text{for } j = 1, 2 \quad (7)$$

Note that this equation results in $f_c > 1$ if $\delta_j < t_j$ or $f_c = 1$ if no axial constriction exists in the outer ring when $\delta_j = t_j$. Also, $\alpha = \pi/4$ and the outer radius of the plate, b , is related to the square plate dimension L as follows.

$$b = \frac{L}{\sqrt{\pi}} \quad (8)$$

All of the above resistances are obtained based on the average temperature rise of the source surface over that of the sink surface. The total resistance of a plate is the sum of R_i and R_o , and the total joint resistance of the upper and lower plates is the sum of the resistances of the individual plates:

$$R_t = (R_i + R_o)_1 + (R_i + R_o)_2 \quad (9)$$

where the subscripts 1 and 2 correspond to the upper and lower plates, as in t_1 and t_2 .

The above resistances, R_m and R_t , have been computed for various cases with a set of plates having different thicknesses and different contact radii. Polynomial approximations (Abramowitz and Stegun, 1970) are used in evaluating the Bessel functions. It typically requires about 20 terms of the series solutions to obtain a resistance value with a 4 decimal place accuracy.

The results obtained for the cases where two mating plates are of the same thickness, $t_1 = t_2$, are presented first. They are plotted in Figs. 3 through 9 as functions of contact radius c . It is to be mentioned that, by using dimensionless variables, all the analytical predictions presented in this paper can be collapsed into a narrow range, and many plots may possibly be combined into a single one. However, the dimensional plots are presented here to allow the cases to be compared separately with better clarity. Figures 3 to 8 display the curves obtained for copper plates ($k = 398$ W/mK) with six different thicknesses ranging from $t = t_1 = t_2 = 1.59$ to 12.7 mm, and Fig. 9 shows the results obtained for a set of stainless steel plates ($k = 19$ W/mK) of 1.59 mm thick. All the cases examined herein have a fixed bolt-hole size of 2 mm radius

and the plate dimension $L = 25.4$ mm. The material resistance R_m is independent of the contact radius and, therefore, shown in the figures as a constant function.

Also included in the figures are the finite element predictions and the data obtained from the correlation equation of Song et al. (1993a):

$$R_J = \frac{1}{kt} \left[\frac{\sqrt{tL}}{\pi c} + \frac{1}{2} \right] \quad (10)$$

which is shown to be in good agreement with the numerical results. In addition, the experimentally measured total joint resistances reported by Song et al., (1993a) are compared in Figs. 3 to 6. The measured values agree well with the predictions obtained from either the numerical method or the above correlation equation when the plate thickness and the contact area are large. However, the agreement becomes poor as the plate thickness and/or the contact area becomes small.

As discussed in the previous section, it is clearly revealed in the figures that R_m represents the minimum resistance to which the total system resistance approaches as the contact radius increases, and R_t represents the total system resistance at small contact radii. These two limiting resistances, representing the asymptotic values of the total joint resistance, can be blended (Churchill and Chu, 1975) to correctly yield the total joint resistance R_J as follows:

$$R_J = \left[R_t^n + \left(R_m \frac{c-a}{b-a} \right)^n \right]^{1/n} \quad (11)$$

with the blending exponent $n = 1.5$. Recall that, in the limit as the contact area becomes small, R_t is R_J . Therefore, as $c \rightarrow a$, a full contribution of R_m to R_J is not necessary and, to reflect this through the blending, R_m is down-weighted by a factor $(c-a)/(b-a)$, as shown in the above equation. This factor pro-

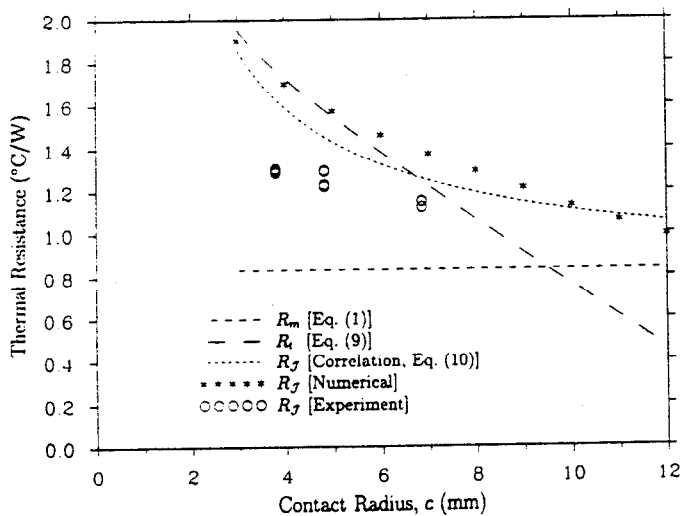


Figure 3: Thermal Resistance versus Contact Radius for Copper Plates of Equal Thickness ($k = 398$ W/mK, $t_1 = t_2 = 1.59$ mm)

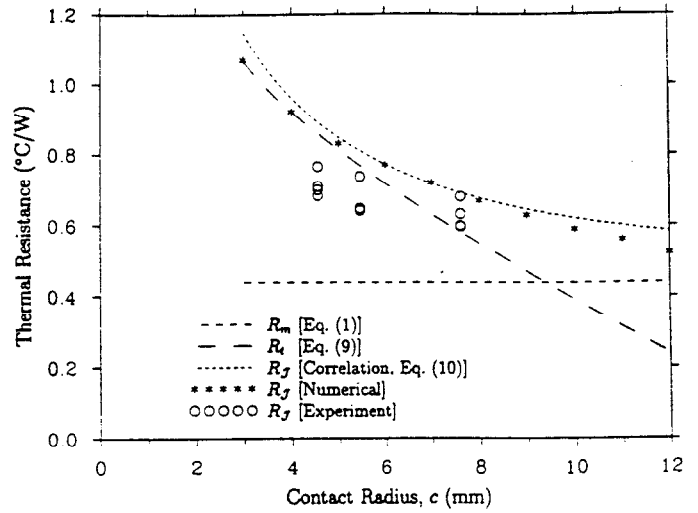


Figure 4: Thermal Resistance versus Contact Radius for Copper Plates of Equal Thickness ($k = 398$ W/mK, $t_1 = t_2 = 3.18$ mm)

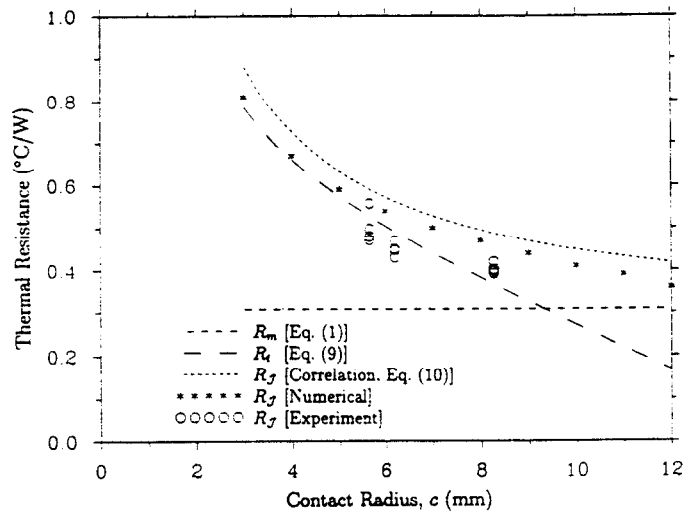


Figure 5: Thermal Resistance versus Contact Radius for Copper Plates of Equal Thickness ($k = 398$ W/mK, $t_1 = t_2 = 4.76$ mm)

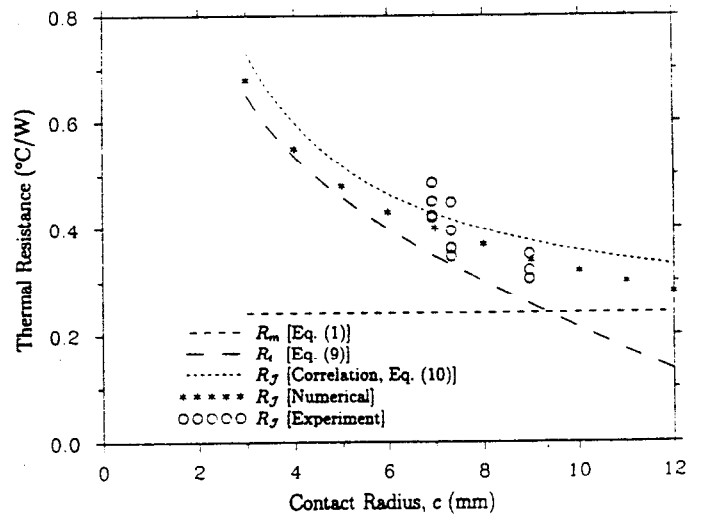


Figure 6: Thermal Resistance versus Contact Radius for Copper Plates of Equal Thickness ($k = 398$ W/mK, $t_1 = t_2 = 6.35$ mm)

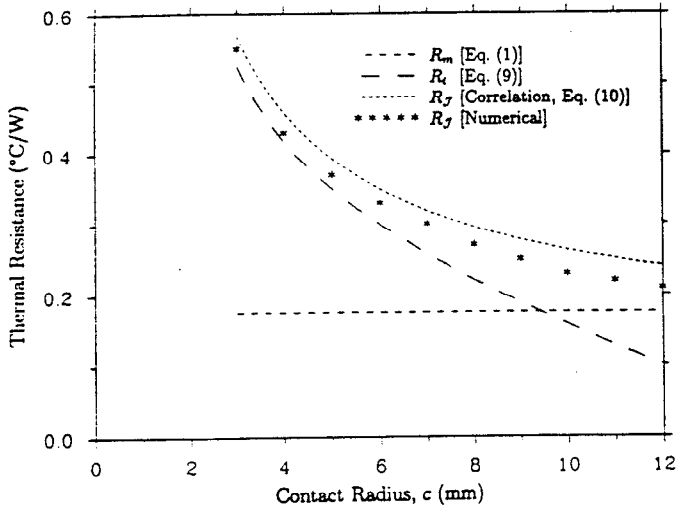


Figure 7: Thermal Resistance versus Contact Radius for Copper Plates of Equal Thickness ($k = 398 \text{ W/mK}$, $t_1 = t_2 = 9.53 \text{ mm}$)

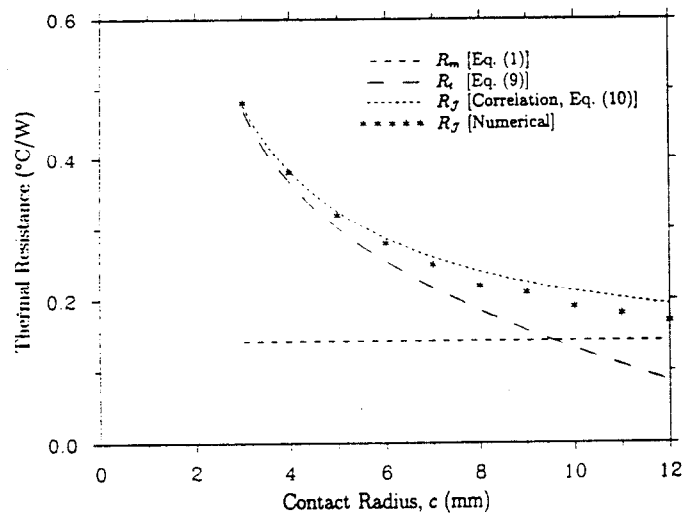


Figure 8: Thermal Resistance versus Contact Radius for Copper Plates of Equal Thickness ($k = 398 \text{ W/mK}$, $t_1 = t_2 = 12.7 \text{ mm}$)

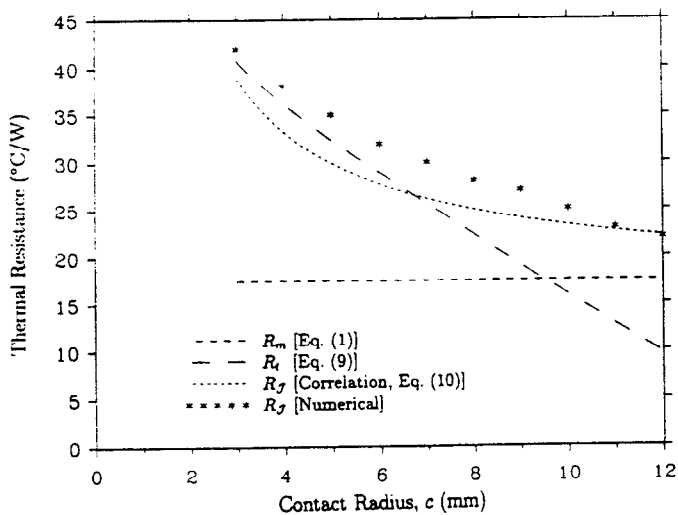


Figure 9: Thermal Resistance versus Contact Radius for Stainless Steel Plates of Equal Thickness ($k = 19 \text{ W/mK}$, $t_1 = t_2 = 1.59 \text{ mm}$)

gressively reduces the contribution of R_m as the contact radius becomes small. The above blended solution is compared with the numerical results in Fig. 10 for the previous cases with copper plates and in Fig. 11 for the stainless steel case. As can be seen from the figures, the comparisons resulted in excellent agreement.

Song and his co-workers (1993b) further investigated the similar problem involving bolted joints between two plates of unequal thickness. They provided experimental results for various combinations of plates with different thicknesses, and extended their correlation equation, Eq. (10), initially developed for the equal thickness problem, to include the cases with unequal thickness. This correlation is rewritten here as

$$R_J = \frac{1}{k} \left[\frac{\sqrt{L}}{2\pi c} \left(\frac{1}{\sqrt{t_1}} + \frac{1}{\sqrt{t_2}} \right) + \frac{1}{2t_h} \right] \quad (12)$$

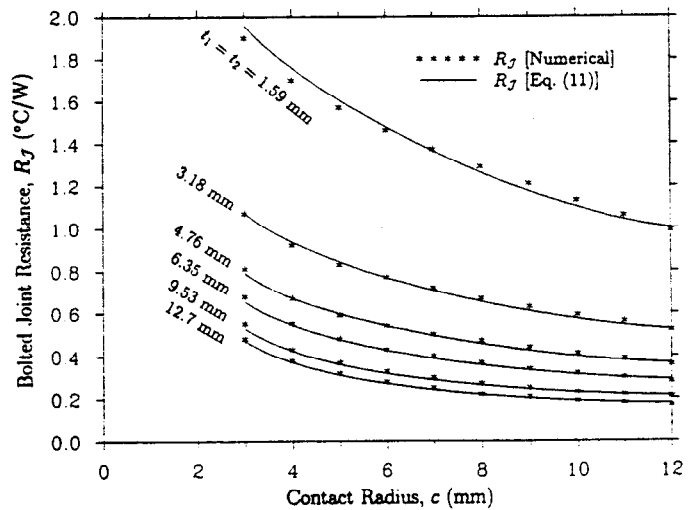


Figure 10: Comparison of Bolted Joint Resistances for Copper Plates of Equal Thickness

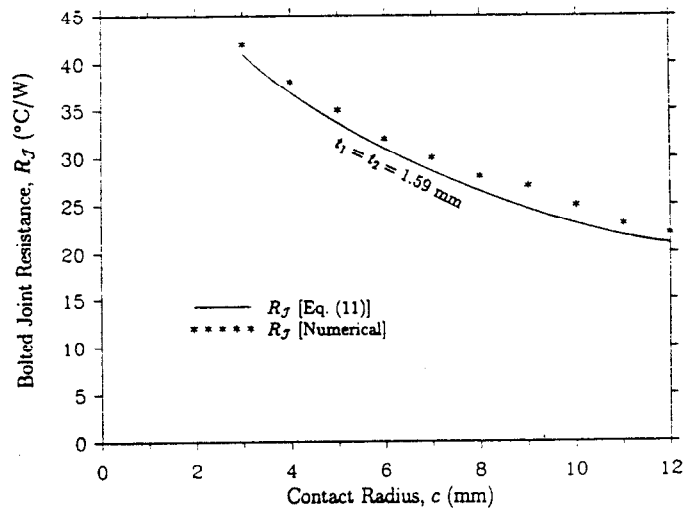


Figure 11: Comparison of Bolted Joint Resistances for Stainless Steel Plates of Equal Thickness

where t_h is the harmonic mean thickness of the two plates, defined as

$$t_h = \frac{2t_1t_2}{t_1 + t_2} \quad (13)$$

Also, an experimentally based correlation equation was provided for accurate estimation of the contact radius c as

$$c = d + \frac{t_h}{2} \quad (14)$$

where d denotes the washer or pressure radius of the bolted joint (see Fig. 1b). It is to be noted that, when $t_1 = t_2$, Eq. (12) reduces to Eq. (10).

The various resistances, including R_m and R_t given by Eqs. (1) and (9), and the total joint resistances computed from Eqs. (11) and (12) are presented in Figs. 12 through 17 as a function of the washer radius d for a variety of combinations of different plate thicknesses. The contact radius c , required in computing R_m and R_t , is obtained from Eq. (14). Again, the bolt-hole radius for these cases is fixed at 2 mm and the plate dimension $L = 25.4$ mm. The experimental data of Song et al. (1993b) are also included in the figures. The measured values display the similar behavior previously observed in the equal thickness cases: a greater deviation from the analytical and correlated predictions as the washer radius (therefore the contact radius) and/or the plate thickness become small. In general, the agreement between the correlations and the present analytical predictions is good.

An attempt was made to develop an "improved" correlation equation by utilizing the parametric groups appeared in the analytical solutions. However, new expressions are found to be no superior to the existing correlation given by Eq. (12) in terms of its simplicity and accuracy. For this reason, no other correlation is proposed as a result of this study.

CONCLUSIONS

The thermal resistance of a bolted joint between two concentric square plates has been investigated. The mating plates are of the same material but may be of different thicknesses. For thermal analyses, it is assumed that the annular contact area at the interface is given, and the plate surfaces are smooth and the contact is perfect. Due to the lack of an orthogonal coordinate system that conforms to the geometry and thermal boundary conditions of the present problem, an approximate approach has been employed to develop a simple, closed form expression for the total joint resistance. The final expression is obtained in the form of a blended equation using the two asymptotic solutions, each of which represents the correct limit of the joint resistance as the contact area becomes either large or small. The results are presented over a wide range of parameters including equal and unequal plate

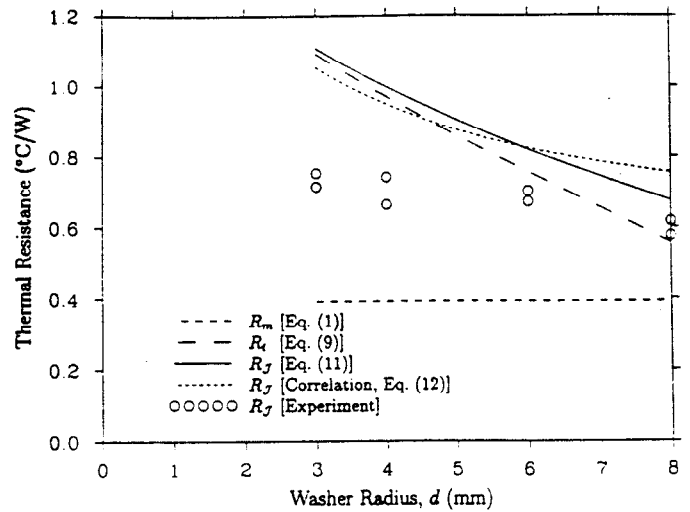


Figure 12: Thermal Resistance versus Washer Radius for Copper Plates of Unequal Thickness ($k = 398$ W/mK, $t_1 = 1.59$ mm, $t_2 = 6.35$ mm)

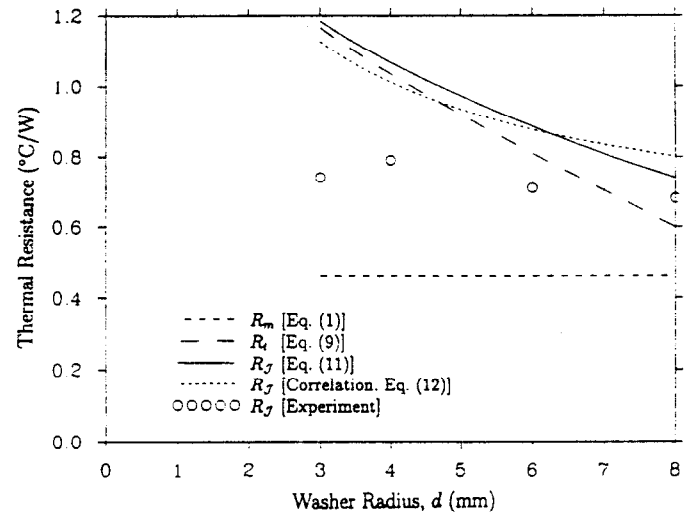


Figure 13: Thermal Resistance versus Washer Radius for Copper Plates of Unequal Thickness ($k = 398$ W/mK, $t_1 = 1.59$ mm, $t_2 = 4.76$ mm)

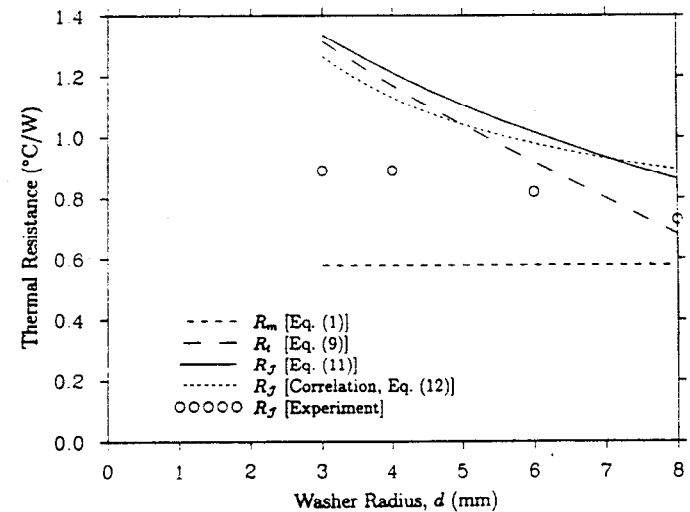


Figure 14: Thermal Resistance versus Washer Radius for Copper Plates of Unequal Thickness ($k = 398$ W/mK, $t_1 = 1.59$ mm, $t_2 = 3.18$ mm)

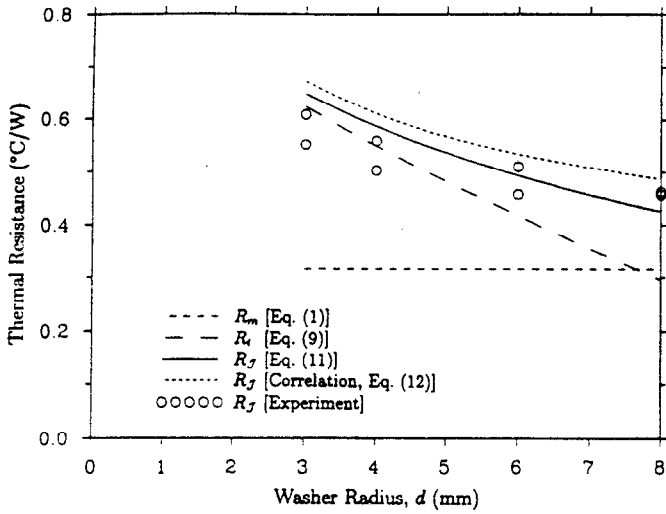


Figure 15: Thermal Resistance versus Washer Radius for Copper Plates of Unequal Thickness ($k = 398 \text{ W/mK}$, $t_1 = 3.18 \text{ mm}$, $t_2 = 6.35 \text{ mm}$)

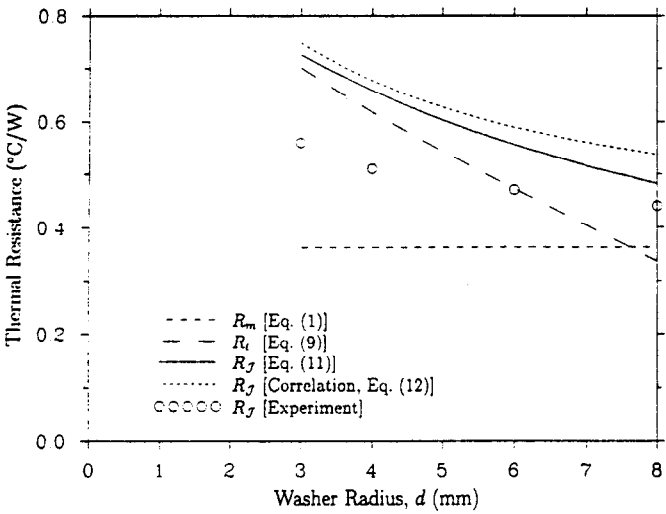


Figure 16: Thermal Resistance versus Washer Radius for Copper Plates of Unequal Thickness ($k = 398 \text{ W/mK}$, $t_1 = 3.18 \text{ mm}$, $t_2 = 4.76 \text{ mm}$)

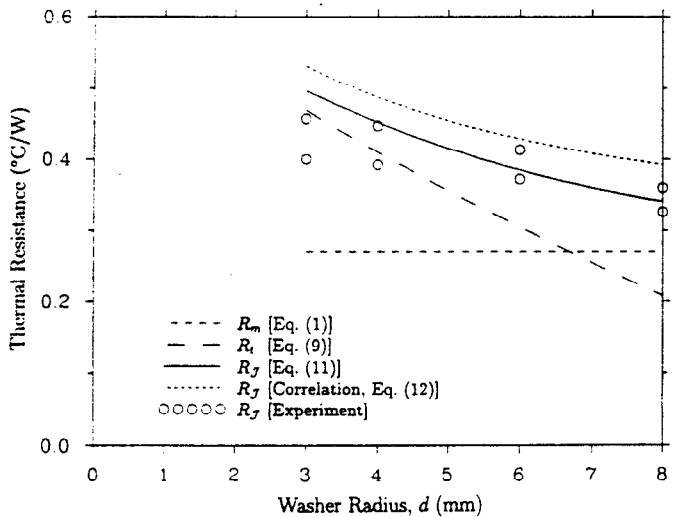


Figure 17: Thermal Resistance versus Washer Radius for Copper Plates of Unequal Thickness ($k = 398 \text{ W/mK}$, $t_1 = 4.76 \text{ mm}$, $t_2 = 6.35 \text{ mm}$)

thicknesses, the plate thermal conductivity and the contact radius. Comparisons of the present analytical predictions with existing finite element data resulted in excellent agreement. However, the available experimental measurements show limited agreement with both the numerical and present approximate solutions. It was concluded that the existing simple correlation equation is adequate in predicting the joint resistance over the range of parameters examined in this paper.

REFERENCES

- Abramowitz, M., and Stegun, I.A., 1970, *Handbook of Mathematical Functions*, Dover Publications, New York.
- Churchill, S.W., and Chu, H.H.S., 1975, "Correlating Equations for Laminar and Turbulent Free Convection From A Horizontal Cylinder," *Int. J. Heat Mass Transfer*, Vol. 18, pp. 1049-1053.
- Lee, S., Lemczyk, T.F., and Yovanovich, M.M., 1992, "Analysis of Thermal Vias in High Density Interconnect Technology," Proceedings of the 8th Annual IEEE Semiconductor Thermal Measurement and Management Symposium, pp. 89-94.
- Lee, S., Yovanovich, M.M., Song, S., and Moran, K.P., 1993, "Analysis of Thermal Constriction Resistance In Bolted Joints," *The International Journal of Microcircuits and Electronic Packaging*, Vol. 16, No. 2, pp. 125-136.
- Song, S., Moran, K.P., Augi, R., and Lee, S., 1993a, "Experimental Study and Modeling of Thermal Contact Resistance Across Bolted Joints," AIAA Paper No. 93-0844. Also, to appear in the *Journal of Thermophysics and Heat Transfer*.
- Song, S., Moran, K.P., and Lee, S., 1993b, "Thermal and Electrical Resistances of Bolted Joints Between Plates of Unequal Thickness," Proceedings of the 9th Annual IEEE Semiconductor Thermal Measurement and Management Symposium, IEEE Catalog No. 93CH3226-8, pp. 28-34.
- Song, S., Park, C., Moran, K.P., and Lee, S., 1992, "Contact Area of Bolted Joint Interface: Analytical, Finite Element Modeling, and Experimental Study," Proceedings of the 1992 ASME Winter Annual Meeting, EEP-Vol 3, pp. 73-81.
- Yovanovich, M.M., 1992, *Thermal Contact Resistance: Theory and Applications*, Course Notes, Department of Mechanical Engineering, University of Waterloo.